PHASE DETECTION IN A VISUAL-EVOKED-POTENTIAL BASED BRAIN COMPUTER INTERFACE

Gary Garcia Molina, Danhua Zhu, and Shirin Abtahi

Philips Research Europe
High Tech Campus 34, 5656AE, Eindhoven, The Netherlands
phone: + (31) 402747959, { gary.garcia, zhu.danhua, shirin.abtahi }@philips.com

ABSTRACT

Brain-computer interfaces (BCI) based on Steady State Visual Evoked Potential (SSVEP) can provide higher information transfer rate than other BCI modalities. For the sake of safety and comfort, the frequency of the repetitive visual stimulus (RVS) necessary to elicit an SSVEP, should be higher than 30 Hz. However, in the frequency range above 30 Hz, only a limited number of frequencies can elicit sufficiently strong SSVEPs for BCI purposes. Consequently, the conventional approach, consisting in presenting various repetitive visual stimuli having different frequency each, is not practical for SSVEP based BCI functioning. Indeed this would bring low communication bitrates. In order to increase the number of possible repetitive visual stimuli, we consider modulating the phase of the stimulus instead of the frequency. Thus, several stimuli, sharing the same frequency, but with different phase can be presented to the user. The approach presented in this document, to detect the phase of the stimulus is termed phase synchrony. It consists in using as feature, the phase difference between the SSVEP and the stimulus. The phase is extracted through the Hilbert transform applied on an univariate signal resulting from spatially filtering the electroencephalogram. The spatial filter is determined in such a way that the SSVEP energy is enhanced through a linear combination of the signals recorded at different positions on the scalp. Phase detection accuracy for seven subjects ranges from 70 to 94%.

1. INTRODUCTION

The steady state visual evoked potential (SSVEP) refers to the response of the cerebral cortex to a repetitive visual stimulus (RVS) oscillating at a constant frequency. The SSVEP manifests as an oscillatory component in the electroencephalogram (EEG) having the same frequency (and/or harmonics) as the RVS [1]. Because of their proximity to the primary visual cortex, the occipital sites exhibit a higher SSVEP response. The EEG is typically recorded using an array of electrodes positioned according to the 10-20 system [2] (Figure 1a).

The SSVEP is an effective electrophysiological source that can be used as input for brain computer interfaces (BCI) [3]. An SSVEP based BCI operates by presenting the subject with a set of repetitive visual stimuli (RVSi). In general, the RVSi oscillate at different frequencies from each other [4]. The SSVEP corresponding to the RVS on which the subject focuses his/her attention is more prominent and can be detected from the ongoing EEG. Each RVS is associated with an action which is executed by the BCI system when the corresponding SSVEP is detected.

SSVEP based BCIs offer two main advantages over BCIs based on other electrophysiological sources (e.g. P300, ERD/ERS): i) have higher information transfer rate, and ii) require shorter calibration time [5].

Most SSVEP-based BCIs use stimulation frequencies in the 4-30 Hz range [6]. SSVEPs elicited by frequencies in this range have high amplitude but can lead to visual fatigue or even induce epileptic seizures [7]. For safety and comfort, higher stimulation frequencies are therefore preferable. However, only a limited number of frequencies above 30 Hz can elicit a sufficiently strong SSVEP for BCI purposes (see Section 4). Thus, if a frequency per target is used, the number of choices (and consequently the information transfer rate) in a BCI is limited.

A possible manner to tackle such limitation consists in combining several frequencies to drive a single visual stimulus [8, 9]. Thus, if N frequencies are used, a target may combine k frequencies selected among the available N. From combinatory theory it is known that $\binom{N}{k} > N$ if $N > k+1$ and $k > 1$. An alternative manner consists in using the same frequency for several stimuli but different phase [10, 11]. Detecting the phase of the stimulus that receives the user's focus of attention is possible because the SSVEP is phase-locked with the stimulus [1].

The SSVEP phase can be obtained using methods based on the Discrete Fourier Transform [10, 11, 12]. However, these methods require relatively long signal segments containing a number of samples that is a multiple of the stimulus period. This increases the latency period and therefore reduces the information transfer rate.

In this paper, the phase is detected using the Hilbert transform. To align the stimulus with the SSVEP, the oscillatory light emanating from one of the stimuli was simultaneously recorded (without loss of generality, the stimulus with 0-phase was selected). In the following we refer to such a signal as *stimulation-signal*.

This paper is organized as follows. The experimental protocol is described in Section 2, then the signal processing methods are presented in Section 3. The evaluation of results are discussed in Section 4. The conclusion and future directions are presented in Section 5.

2. EXPERIMENTAL PROTOCOL

Four 10×10 cm luminous panels positioned around a 20-inch computer screen were used to render the visual stimuli. Each panel consisted of a 1-watt power green LED shinning through a diffusion panel. The LED was driven by a square-shaped oscillating current. The maximum luminance of each

 ISSN 2076-1465

LED was 1714 nits. The background luminance was 69.7 nits which corresponds to an office environment illuminated with artificial light and closed curtains.

Subjects were seated on a chair 70 cm away from the luminous panels. The panels rendered repetitive visual stimuli at the same frequency (which was the optimal stimulation frequency for each subject, see Table 1) and phases 0, $\pi/2$, π, and $3\pi/2$.

The optimal stimulation frequency for each subject was determined by: *i*) presenting stimuli at all integer frequencies from 30 to 40 Hz, *ii*) recording the corresponding SSVEPs and identifying the frequency which elicited the highest SSVEP. Seven subjects (two female and five male) participated in this study. Five subjects had normal vision and the other two used correcting glasses. All subjects signed an informed consent before engaging in this study and had the right to quit at any time.

Subjects were asked to pay attention to one out of the four luminous panels for 3 seconds. This 3-second long period as referred to as *trial*. For each subject, we recorded 160 trials separated from each other by a resting period of a random duration between 3 and 5 seconds. Each subject participated in four recording sessions which lasted for about 30 minutes each and were conducted during different days. During each trial, subjects were asked to focus their attention on a randomly selected panel. The random sequence was such that it resulted in equal number of trials (i.e. 40) per phase condition.

EEG signals were collected using a BioSemi acquisition system [13] in a normal office environment. Signals from 8 electrode locations: P3, Pz, P4, PO3, PO, O1, Oz, and O2 referenced to Cz were recorded at a sampling frequency of 2048 Hz (see [2] for the standard EEG electrode positioning and Figure 1a). During the trials, subjects were requested to avoid movement or eye-blinking while they were encouraged to blink during the resting period between two consecutive trials.

The light signal from the 0-phase panel was simultaneously recorded using a photodiode connected to the EEG acquisition device. Such signal constitutes the stimulation-signal that is used to detect the SSVEP phase (Section 3.2).

3. SIGNAL PROCESSING METHODS

A signal recorded at a particular electrode location, that contains T samples can be seen as a vector in $\mathbb{R}^T$. Because of this interpretation, we use hereafter the terms vector and signal without explicit distinction.

The EEG signal $\vec{x}_i$ (where i indexes the electrode location) recorded while the subject focuses on an RVS at a frequency f and phase θ can be written as a sum of the SSVEP component (denoted as $\vec{s}_i$), background EEG, and noise [14]. For convenience the background EEG and the noise at electrode i are combined into a single term denoted as $\vec{y}_i$. Thus, the following relation holds (see also Figure 1b).

$$\begin{aligned}\vec{x}_i &= \vec{s}_i + \vec{y}_i \\ &= \sum_{h=1}^{H} \left(a_{h,i}\sin(2\pi h f\vec{t}+\theta) + b_{h,i}\cos(2\pi h f\vec{t}+\theta)\right) + \vec{y}_i,\end{aligned} \tag{1}$$

where the SSVEP component is modeled as a linear combination of vectors in the set:

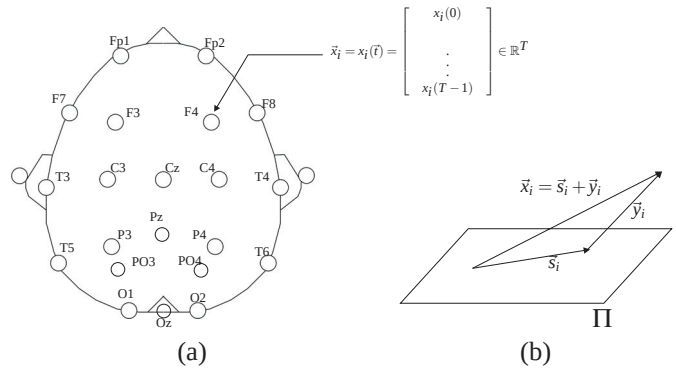

Figure 1: (a) 10-20 EEG electrode positioning system. (b) Vector interpretation of the recorded signals and the space Π of SSVEP components.

$\Phi = \{\sin(2\pi h f\vec{t}), \cos(2\pi h f\vec{t}) \,|\, h = 1,\ldots,H\}$, $\vec{t} = [0,\ldots,T-1]'$ is a vector of sample indices, H is the number of harmonics that are considered in the model, and $a_{h,i}, b_{h,i}$ are real numbers. In (1), it is assumed that the phase of the RVS equally affects all the recorded signals. While this assumption may not hold for electrode sites located far from each other, it does hold when the signals are recorded from electrodes that are relatively close to each other. In particular in our study, where the signals originate from electrodes in the proximity of the primary visual cortex (see Section 2).

Equation 1 can be generalized to the whole set of electrodes $\{\vec{x}_i \,|\, i = 1,\ldots,N\}$ (N being the number of electrodes) in the following matrix form:

$$X = S\Theta A + Y, \tag{2}$$

where the matrix $X \in \mathbb{R}^{T\times N}$ has as columns the vectors $\vec{x}_i$, $Y \in \mathbb{R}^{T\times N}$ has as columns the vectors $\vec{y}_i$, $S \in \mathbb{R}^{T\times 2H}$ has as columns the vectors in the set Φ, $\Theta = \begin{pmatrix} \cos\theta & -\sin\theta \\ -\sin\theta & -\cos\theta \end{pmatrix}$, and $A \in \mathbb{R}^{2H\times N}$ is the matrix of linear combination coefficients such that $A_{h,i} = a_{h,i}$ if h is odd and $A_{h,i} = b_{h,i}$ if h is even. By means of the coefficients $a_{h,i}$ and $b_{h,i}$, the model in (2) takes into account the differences of SSVEP-strength across the scalp.

3.1 SSVEP enhancement through spatial filtering

This section summarizes the spatial filtering technique for SSVEP enhancement presented in [14, 15].

The elements of A and the phase θ in (2) cannot be determined from X and S only. Thus, to determine the SSVEP strength at different electrode locations, a vector $\vec{x}_w$ is constructed such that: $\vec{x}_w = \sum_i w_i\vec{x}_i = X\vec{w}$, where $\vec{w} = [w_1,\ldots,w_N]'$. The vector $\vec{x}_w$ can be considered to be the result of a spatial filter (e.g., filtering across the electrodes) with coefficients $\{w_i\}$ applied to the measured signals $\vec{x}_i$. The spatial filter is determined in such a way that it simultaneously maximizes the energy in the SSVEP frequencies and minimizes the energy elsewhere [15, 16]. This ratio can be determined by relying on the following geometric interpretation.

The columns of S (i.e. vectors in the set Φ) are linearly independent and so the columns of $S\Theta$ (i.e. the phase shifted versions of vectors in Φ). The columns of $S\Theta$ generate a

vector space of dimension $2H$ which we denote as Π. We assume Π to be the space where the SSVEP components lie (Figure 1b). Under this assumption, Π's orthogonal complement $\Pi^{\perp}$ contains the non-SSVEP components. Since the columns in $S\Theta$ are linearly independent, the projection matrix Q on Π can be written as $Q = S\Theta\left(\Theta' S' S\Theta\right)^{-1}\Theta' S'$ [17]. Following straightforward algebra manipulations, it can be seen that $Q = S\Theta\Theta^{-1}\left(S'S\right)^{-1}\left(\Theta'\right)^{-1}\Theta' S' = S\left(S'S\right)^{-1}S'$. Thus, the projection matrix is independent of the phase.

The component of $X\vec{w}$ in $\Pi^{\perp}$ is equal to $X\vec{w} - QX\vec{w}$. The Euclidean norm of the latter: $\|(X-QX)\vec{w}\|^2$ divided by T represents the power of the non-SSVEP related activity. The power of the SSVEP related activity can be approximated by $\|X\vec{w}\|^2$. The spatial filter $\vec{w}$ corresponds to the argument that maximizes the ratio $\rho = \frac{\vec{w}'X'X\vec{w}}{\|(X-QX)\vec{w}\|^2}$,

$$\vec{w} = \arg\max_{\tilde{\vec{w}}} \frac{\tilde{\vec{w}}' X' X \tilde{\vec{w}}}{\tilde{\vec{w}}'(X-QX)'(X-QX)\tilde{\vec{w}}}. \tag{3}$$

The ratio in (3) is a generalized Rayleigh quotient [18] whose maximum can be found through a generalized eigendecomposition of the matrices $X'X$ and $(X-QX)'(X-QX)$. This results into two matrices $W, \Lambda \in \mathbb{R}^{N\times N}$ such that,

$$X'X = (X-QX)'(X-QX)W\Lambda, \tag{4}$$

where Λ is a diagonal matrix whose diagonal contains the eigenvalues. The corresponding eigenvectors are in the columns of W. By construction, eigenvalues are larger than one [19]. The largest element in Λ corresponds to the maximum of the quotient in (3). The column of W corresponding to such maximum is the sought spatial filter $\vec{w}$.

Given that high frequency stimulation is applied, and the limited spectrum of EEG signals, we consider only the stimulation frequency in our model (2) and disregard higher harmonics. Thus, $H = 1$ is used to calculate Q.

In this study, we used the calibration strategy detailed in [15] to obtain $\vec{w}$. Using these coefficients we obtain the vector (univariate signal), $\vec{x}_w$.

For convenience of presentation of the phase synchrony analysis in next Section 3.2, we refer to $\vec{x}_w$ in terms of its time domain representation $x_w(t)$.

3.2 Phase synchrony analysis

The instantaneous phases at the stimulation frequency of the stimulation-signal $l(t)$ (recorded as explained in Section 2), and $x_w(t)$ can be estimated by using the Hilbert transform [20]. Thus, $l(t)$ and $x_w(t)$ are first filtered by a 1-Hz wide bandpass linear-phase FIR filter centered at the stimulation frequency. This results in the signals $\tilde{l}(t)$ and $\tilde{x}_w(t)$ which are the bandpass filtered versions of $l(t)$ and $x_w(t)$ respectively. The corresponding analytical signals are [20]:

$$\begin{aligned} A_x(t) &= \tilde{x}_w(t) + j\mathscr{H}\{\tilde{x}_w(t)\} &= R_x(t)e^{j\theta_x(t)} \\ A_l(t) &= \tilde{l}(t) + j\mathscr{H}\{\tilde{l}(t)\} &= R_l(t)e^{j\theta_l(t)} \end{aligned} \tag{5}$$

where $\mathscr{H}\{\tilde{x}_w(t)\}$, $\mathscr{H}\{\tilde{l}(t)\}$ are the Hilbert transforms of $\tilde{x}_w(t)$ and $\tilde{l}(t)$.

The phase difference $\Delta\theta_{x_w,l}(f,t)$ at frequency f and time t between the SSVEP and the stimulation-signal can be obtained from:

$$\begin{aligned} \Delta\theta_{x_w,l}(f,t) &= \arg\{e^{j(\theta_x(t)-\theta_l(t))}\} \\ &= \arg\left\{\frac{A_x(t)A_l^*(t)}{\|A_x(t)\|\|A_l^*(t)\|}\right\} \end{aligned} \tag{6}$$

where * operator stands for the complex conjugate. In practice, the phase is estimated within a time window. From a τ-sample long window, we estimate the phase difference within that particular window as the mode of the distribution resulting from the τ phase differences.

4. RESULTS

Table 1 reports the optimal stimulation frequency (Stim. freq.) for each subject. In addition, Figure 2 depicts the distribution of the SSVEP energy for integer stimulation frequencies (from 30 to 40 Hz) for subjects S1 (Figure 2a) and S2 (Figure 2b). The boxplots resulted from forty trials. Subject S1 exhibits a decreasing trend of the SSVEP for increasing stimulation frequencies. Subject S2 has a maximum SSVEP at 31 Hz and does also exhibit a decreasing trend for the SSVEP amplitude for increasing stimulation frequencies starting from 31 Hz. Such trend is not present in all subjects since subjects S3, S4, S5, and S7 have optimum stimulation frequencies higher than 35 Hz.

Figure 3 shows the phase difference between the SSVEP and the light signal extracted from 1-second long EEG segment recorded while the attention of subject S1 was focused on the panel with 0-phase (thick line) and on the panel with π-phase (dashed line). It is clear that the phase difference can be extracted by the phase synchrony analysis as it fluctuates around a constant value. The measured phase difference values can, therefore, be used to identify which panel received the subject's attention.

We used the algorithm discussed in Section 3.1 to obtain the spatial filters for each subject. The spatial filters can be represented in a topographic map as shown in Figure 4. Given that each coefficient of the filter is associated with an electrode location, it can be represented using a color code which facilitates the interpretation of the result. Although only 8 coefficients (corresponding to the recorded electrodes) were calculated, the topographic map for the whole head (with zero values for sites other than the recorded ones) is shown for convenience of representation. Subject variability of the spatial filters is clear from Figure 4.

Two phase differences were estimated per trial. These corresponded to the one-second long windows starting one second, and two seconds after stimulus onset respectively. The first second of each trial was discarded because the SSVEP establishes few hundred milliseconds after stimulus onset [1].

To estimate the detection accuracy and the prospective information transfer rate, a four-class single layer neural network with four input neurons and four output neurons was trained with half of the available data. This means 4×40 phase-differences per phase condition. The average detection accuracy was then determined and is reported in Table 1 for each subject. Assuming that the probability of attention focus on each of the four panels is equal, the following formula can be used to estimate the information transfer rate in bits-per-minute (bpm) [21].

Table 1: Phase detection performance

Subject	Stim. freq. [Hz]	Avg. Detection Accuracy	Bitrate [bpm]
S1	30	0.94	100.9
S2	31	0.86	83.0
S3	39	0.92	96.0
S4	36	0.85	81.1
S5	39	0.71	58.3
S6	32	0.81	73.8
S7	39	0.93	98.3

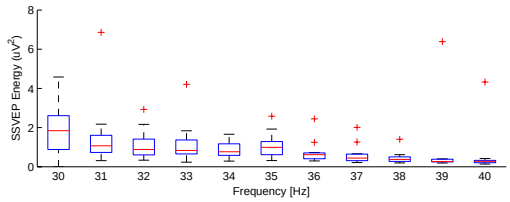

(a)

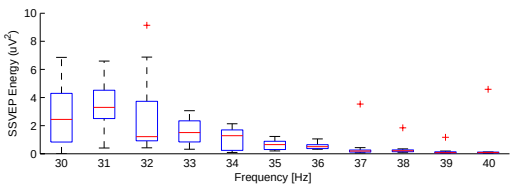

(b)

Figure 2: Boxplot of the SSVEP energy for all integer stimulation frequencies in the 30-40 Hz range for subjects S1 (a) and S2 (b). These distributions were obtained from analyzing forty trials at each stimulation frequency.

$$\text{Bit rate} = 60\left(2 + p_a \log_2 p_a + (1-p_a)\log_2 \frac{1-p_a}{3}\right) \quad (7)$$

where p_a is the average detection accuracy.

Bitrate results are above 70 bpm which ensure smooth interaction for all subjects except S5. These results are highly promising and support the idea of using high frequencies and phase detection to bring SSVEP based BCIs one step further into a practical assistive tool for the physically challenged and the healthy.

5. CONCLUSIONS

The phase synchrony analysis can effectively extract the phase difference between the SSVEP and the light signal.

The difference between these two values deviates slightly from the expected value , but the difference is sufficient for detection. In this study, the Hilbert transform was used to obtain the analytical representation of a signal. In principle, the Hilbert transform can be applied to any arbitrary signal to extract its instantaneous phase. Yet, the phase has a physical meaning only if the signal is a narrow-band signal. This is why we use an FIR filter centered at the frequency of

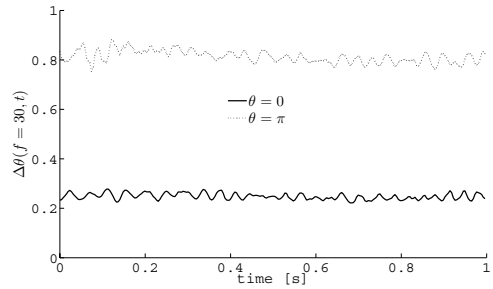

Figure 3: Instantaneous phase difference extracted from a 1-second long EEG recorded while the attention of subject S1 was focused on the panel with 0-phase (thick line) and on the panel with π-phase (dashed line)..

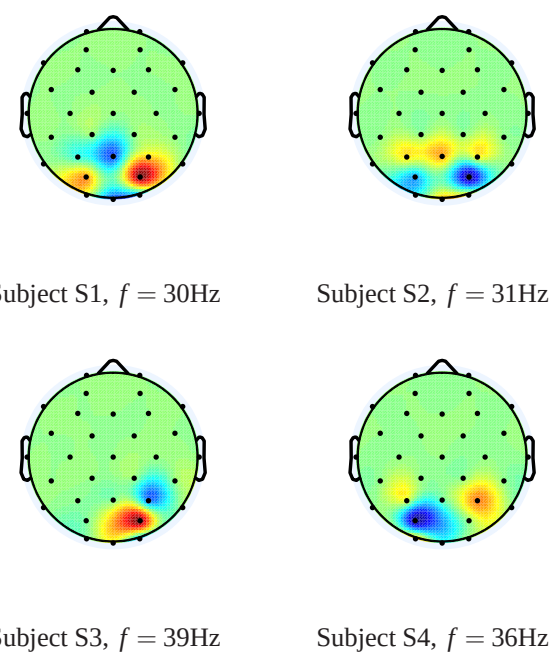

Figure 4: Topographic maps for subjects S1 to S4 at their respective optimum stimulation frequencies (see Table 1).

interest. A Gabor wavelet convolution can alternatively be used to analyze neural synchrony as in [22]. The difference between these two methods is minor and they are fundamentally equivalent for the study of neuroelectrical signals. However, the Hilbert transform is slightly more efficient from the computational viewpoint.

As shown in Table 1, the information transfer rate is for six out of seven subjects larger than 70 bits-per-minute which can ensure smooth BCI operation.

In this study, the coefficients of the spatial filter for each subject are fixed. Thus, the phase difference after spatial filtering is non-linearly and invariably related to the SSVEP phase of the electrode signals which are used to design a spatial filter. The stimulus phase can deviate from the pre-established value, especially if the stimulus is presented for long time. Using the phase difference between the SSVEP and the stimulus signal as a feature can compensate for this deviation, because the SSVEP is phase-locked.

While the results in this paper appear to be highly promising for BCI implementation, it is necessary to implement this algorithm in an actual BCI to assess its suitability for real time operation. In the current experimental platform, the phase shifting is produced by using several computer controlled function generators. In a practical implementation, the space of possible phase shifts may be reduced due to hardware limitations.

REFERENCES

[1] D. Regan. *Human Brain Electrophysiology: Evoked Potentials and Evoked Magnetic Fields in Science and Medicine*. Elsevier, 1989.

[2] H.H. Jasper. The ten-twenty electrode system of the international federation. *Electroencephalography and Clinical Neurophysiology*, 10(1):371–375, 1958.

[3] Y. Wang, X. Gao, B. Hong, C. Jia, and S. Gao. Brain-Computer Interfaces Based on Visual Evoked Potentials. *IEEE Engineering in Medicine and Biology Magazine*, 27(5):64–71, 2008.

[4] M. Cheng and S. Gao. An EEG-based cursor control system. In *Proc. Annu. Int. Conf. IEEE Engineering in Medicine and Biology Soc.*, page 669, 1999.

[5] M. Cheng, X. Gao, S. Gao, and D. Xu. Design and Implementation of a Brain-Computer Interface With High Transfer Rates. *IEEE Transactions on Biomedical Engineering*, 49(10):1181–1186, 2002.

[6] D. Zhu, J. Bieger, G. Garcia Molina, and R.M. Aarts. A survey of stimulation methods used in SSVEP-based BCIs. *Journal of Computational Intelligence and Neuroscience*, In Press, 2010.

[7] R. S. Fisher, G. Harding, G. Erba, G. L. Barkley, and A. Wilkins. Photic-and pattern-induced seizures: a review for the epilepsy foundation of America working group. *Epilepsia*, 46:1426–1441, 2005.

[8] M. Cheng, X. Gao, S. Gao, and D. Xu. Multiple color stimulus induced steady state visual evoked potentials. In *Proceedings of the 23rd Annual International Conference of the IEEE Engineering in Medicine and Biology Society*, volume 2, pages 1012–1014, 2001.

[9] T M Srihari Mukesh, V Jaganathan, and M Ramasubba Reddy. A novel multiple frequency stimulation method for steady state VEP based brain computer interfaces. *Physiological Measurement*, 27:61–71, 2006.

[10] Yijun Wang, Xiaorong Gao, Bo Hong, Chuan Jia, and Shangkai Gao. Brain-computer interfaces based on visual evoked potentials. *IEEE Engineering in Medicine and Biology Magazine*, 27:64–71, 2008.

[11] T. Kluge and M. Hartmann. Phase coherent detection of steady-state evoked potentials: Experimental results and application to brain-computer interfaces. In *Proceedings of the 3rd International IEEE EMBS Conference on Neural Engineering*, pages 425–429, 2007.

[12] John J. Wilson and Ramaswamy Palaniappan. Augmenting a SSVEP BCI through single cycle analysis and phase weighting. In *Proceedings of the 4th International IEEE EMBS Conference on Neural Engineering*, pages 371–374, 2009.

[13] Biosemi. Biosemi system. http://www.biosemi.com.

[14] O. Friman, I. Volosyak, and A. Gräser. Multiple Channel Detection of Steady-State Visual Evoked Potentials for Brain-Computer Interfaces. *IEEE Transactions on Biomedical Engineering*, 54(4):742–750, 2007.

[15] G. Garcia Molina and V. Mihajlovic. Spatial filters to detect Steady State Visual Evoked Potentials elicited by high frequency stimulation: BCI application. *Journal of Biomedizinische Technik / Biomedical Engineering*, In press, 2010.

[16] Ola Friman, Ivan Volosyak, and Axel Gräser. Multiple channel detection of steady-state visual evoked potentials for brain-computer interfaces. *IEEE Transactions on Biomedical Engineering*, 54:742–750, 2007.

[17] Carl Dean Meyer. *Matrix analysis and applied linear algebra book and solutions manual*, 2000. SIAM.

[18] R.E. Prieto. A general solution to the maximization of the multidimensional generalized Rayleigh quotient used in linear discriminant analysis for signal classification. In *Proc. IEEE Int. Conf. Acoustics, Speech and Signal Processing, ICASSP-2003*, 2003.

[19] G. Sewell. *Computational methods of linear algebra*. Wiley-Interscience, 2005.

[20] L. Cohen. *Time-Frequency Analysis*. Prentice Hall, 1995.

[21] J.R. Wolpaw, N. Birbaumer, D.J. McFarland, G. Pfurtscheller, and T.M. Vaughan. Brain-computer interfaces for communication and control. *Clinical Neurophysiology*, 113:767–791, 2002.

[22] M. Le Van Quyen, J. Foucher, J.P. Lachaux, E. Rodriguez, A. Lutz, J. Martinerie, and F.J. Varela. Comparison of Hilbert transform and wavelet methods for the analysis of neuronal synchrony. *Journal of Neuroscience Methods*, 111(2):83–98, 2001.